

Pivoting the spatial dimension for mobile telecom energy-saving

Liyan Xu^{1##}, Yihang Li^{1,2#}, Hang Yin¹, Hongbin Yu¹, Yuqiao Deng¹, Qian Huang^{3*}, Yinsheng Zhou³, Yu Liu^{4*}

Author Information

¹ College of Architecture and Landscape Architecture, Peking University, Beijing 100871, China.

² College of Urban and Environmental Sciences, Peking University, Beijing 100871, China.

³ Service Lab, Huawei Technologies. Shenzhen 518129, China.

⁴ Institute of Remote Sensing and Geographical Information Systems, Peking University, Beijing 100871, China.

Contributions

Liyan Xu, Yihang Li, and Qian Huang conceptualized this study and contributed to the interpretation, manuscript writing, and development. Yihang Li, Hang Yin, Hongbin Yu, and Yuqiao Deng carried out the data processing and analysis. Yinsheng Zhou contributed to the data acquisition and preprocessing. Yu Liu and Liyan Xu supervised the study.

These authors contributed equally in the paper.

Corresponding authors

Correspondence to: Liyan Xu, Qian Huang, and Yu Liu.

Abstract

Improving energy efficiency is vital for the 5G mobile telecommunication network, while the conventional temporal shutdown strategy is exhausting its energy-saving potential. Inspired by the symmetry between the temporal peaks and valleys and the geographical “highlands” and “lowlands” in network traffic, we propose a new strategy for telecom energy-saving pivoting spatial optimization. We showed by the maximum entropy principle that traffic should follow highly skewed spatial distribution forms, and empirically tested that the probability density function of 4G network traffic typically has a power-law form with an exponential parameter no less than 2 in absolute value. Also, the high-traffic areas form stable “highlands” which enable spatial optimization of base station locations for energy-saving. A simplified model hence built yields up to 19.59% energy savings for the 4G network, and 29.68% for a hypothetical 5G network, prominent margins over what the temporal shutdown approach would gain.

Key words

Mobile communication network, energy saving, network traffic, spatial pattern, power-law, 5G

Reducing carbon emission through conserving fossil energy consumption¹ has been one of the major strategies adopted by countries around the world in response to global climate change, and its importance is particularly evident today when energy prices are soaring under the duress of various uncertainties^{2,3}. The power consumption of the world's massive mobile communication network (MCN) constitutes a significant part of energy use⁴. In the 4G era, the electricity costs of base stations and their ancillary facilities account for more than 30% of the enterprise' operating expenses⁵, and this percentage is expected to further increase in the 5G era. This is due to the fact that the 5G network utilizes high-frequency bands to enable high information capacity, which results in a much lower service coverage radius of a single base station (maximum 100-150m)⁶ than that of a 4G base station (about 1-3km)⁷, and consequently requires more base stations. Meanwhile, the power of a typical 5G base station is usually 2-3 times or even higher than that of a 4G one^{4,8}. A simple calculation, therefore, shows that the overall energy consumption of the 5G network is expected to be about one order of magnitude higher than that of 4G.

In the face of the high energy consumption of the MCN, people have been actively pursuing energy-saving approaches. Most of the existing strategies focus on the temporal dimension, and achieve energy saving by shutting down inactive or low-load base stations during non-peak times⁹. The state-of-the-art of such strategies involve complex shutdown operations at the cell, carrier, and symbol levels^{10,11}, and, in yielding considerable energy savings, their energy-saving effect has appeared to be reaching the theoretical and operational limit today^{12,13}. Therefore, it is imperative to explore additional energy-saving potential of the MCN, not only for global carbon emission reduction, but also for the sustainability of the 5G network.

The principle of spatio-temporal symmetry in geography^{14,15} has inspired the possibility of extracting the additional energy-saving potential in MCN from the *spatial* dimension. Conventionally, energy-saving strategies are rooted in the uneven distribution of MCN usage, usually measured by network traffic, along *time*: given that there are peaks and valleys in the traffic time series¹⁶, energy

savings can be achieved by performing shutdowns during the latter. Likewise, the spatial distribution of traffic is also evidently heterogeneous, which should give rise to a similar strategy: to achieve energy savings through optimizing the spatial distribution of base stations, or reducing the number of operating base stations in places with low loads.

The question is how large is the potential for such energy-saving strategies. Answering this question would require an understanding of the spatial distribution laws of the traffic, which to our knowledge is rarely addressed in the existing literature. Nevertheless, the spatial distribution of certain closely related physical quantities, i.e., mobile signaling¹⁷ and population^{18,19}, which is the user of the MCN, exhibit highly skewed patterns. These facts inspire one to hypothesize that the spatial distribution of the traffic should exhibit similar skewed patterns. Indeed, if the skewness is significant, it intuitively implies that high-traffic areas would account for only a small fraction of the space, thus suggesting considerable energy saving potential. And technically, such potential would be realizable given the current "hybrid networking"⁴ strategy in 5G network building.

For a conceptual deduction of the hypothesis, based on the maximum entropy principle²⁰ which is found prevalent in human behavior, the generalized form of the spatial distribution function $P(X)$ of traffic can be derived as follows (see the Methods section for the detailed deduction):

$$P(X = k) = e^{\lambda_0 - 1 + \lambda_1 \cdot c(k)} \quad (1)$$

Where $P(X = k)$ is the probability when the random variable X for the volume of the traffic (in bits) takes the value k ; $c(k)$ denotes the number of people (users) in the spatial location where $X = k$; and λ is the Lagrangian. Overall, this function takes a generalized exponential form, and in the extreme case when the implicit function $c(k)$ takes a logarithmic form, it may be reduced to a power-law function, while other possible forms of $c(k)$ will lead to more skewed distributions (Fig. 1, see the Methods section for details). This means that the spatial distribution of the traffic is indeed likely to be significantly skewed.

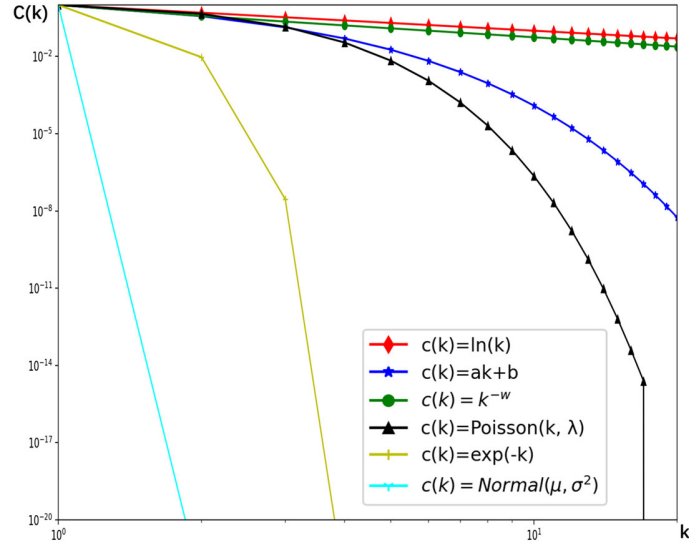


Fig. 1 Possible probability density functions of the spatial distribution of traffic

We test the above hypothesis in the rest of the paper using empirical data by examining the skewness of the spatial distribution of traffic, thereby demonstrating the possibility of an telecom energy-saving strategy based on spatial optimization of base stations. Further, we also use empirical data to validate two important technical prerequisites for the feasibility of the energy-saving strategy, namely 1) the spatial distribution of traffic possesses high spatial autocorrelation with proper characteristic scales, i.e., high traffic areas tend to form continuous clusters in space of which the size matches that of the service coverage radius of base stations, and 2) such spatial structure is stable over time. Finally, we develop a simple spatial optimization model, and show with a set of numerical cases the potentially large energy-saving space of the spatial optimization strategy under typical 4G and 5G network circumstances.

Results

The highly skewed spatial distribution of the MCN traffic

The empirical investigation uses the traffic data from Taiyuan, Shanxi Province, China (see the Methods section for data description). By geographical laws, the spatial distribution of traffic is potentially influenced by the spatial scope²¹ and context²² of analysis. Therefore, we summarized the probability density function (pdf) of the spatial distribution of traffic (daily aggregated) at two granularities: 50 * 50m and 500 * 500m, and at four spatial scales: citywide (~300 km²), district (~ 50 km²), neighborhood (~ 20 km²), and urban place (about 0.2 km²), respectively (Table 1). Results show that: 1) the traffic exhibits a power-law distribution at the citywide scale; as the scale of the analysis going downward, the distribution remains in power-law form in most cases, although in other cases it shows an exponential distribution, or in rare cases a log-normal distribution. 2) At all scales and the 50 * 50m resolution, the α parameters of the power-law distribution form a normal distribution with a mean of 2.3-2.5 and a standard deviation of about 0.36-0.45; in other words, the power-law distributions here are very "steep", and it appears that the smaller the scale is, the steeper the distribution becomes. In the case of the exponential and log-normal distributions, they are even more highly skewed. 3) The above distribution forms appear to be insensitive to the granularity of analysis. At the spatial resolution of 500 * 500m, the mean of α of the power-law distribution is slightly reduced to about 2, and the standard deviation increases to 0.46-0.6, i.e., it still maintains a pattern very similar to that at the 50 * 50m resolution; and the situation is also similar in the case of the exponential and log-normal distributions. Given the above-stated service coverage radiuses of the network, the result indicates that the distributional skewness is meaningful for our energy-saving strategy for both the 4G and 5G networks.

Table 1 Summary of the pdf functions and parameters of the spatial distribution of MCN traffic at multiple spatial scales and granularities

Spatial scope				
pdf of MCN traffic	Citywide (1 Unit of Analysis)	District (6 Units of Analysis)	Neighborhood (12 Units of Analysis)	Urban Place (1228 Units of Analysis)
Granularity = 500 * 500m	Power-law $\alpha = 2.5235$	Power-law (66.6%) $\mu_\alpha = 2.3103$ $\sigma_\alpha = 0.4447$	Power-law (53.84%) $\mu_\alpha = 2.3979$ $\sigma_\alpha = 0.3635$	Power-law (45.78%) $\mu_\alpha = 2.3661$ $\sigma_\alpha = 0.4377$
		others: Exponential (33.4%)	others: Exponential (38.46%); Log-normal (7.69%)	others: Exponential (54.22%)
Granularity = 50 * 50m	Power-law $\alpha = 2.5992$	Power-law (66.6%) $\mu_\alpha = 2.0573$ $\sigma_\alpha = 0.5456$	Power-law (61.5%) $\mu_\alpha = 1.9532$ $\sigma_\alpha = 0.4687$	Power-law (49.3%) $\mu_\alpha = 2.1051$ $\sigma_\alpha = 0.5982$
		others: Exponential (33.4%)	others: Exponential (38.5%)	others: Exponential (50.7%)

Existence of stable MCN traffic “highlands”

Dispite the above-found highly skewed spatial distribution of traffic, two crucial technical prerequisites remain to be met in order to realize the spatial optimization energy-saving strategy. First, the high traffic areas should tend to form continuous spatial clusters of reasonable size. The condition is

necessary because the shutdown of base stations can only be performed in the spatial unit of a cell, and therefore the scale of the high traffic areas must match with the characteristic scale of the cell's service coverage radius. In other words, if the former are so spatially dispersed that each of them occupies only a fraction of a cell, any shutdown operation will affect both high and low traffic areas and thus will not yield significant energy-saving effect. Here, from a geographic perspective, we are actually talking about the autocorrelation nature of the spatial distribution of traffic. Fortunately, calculations show that in the previous case, traffic exhibits significant spatial autocorrelation, with a global Moran's I of 0.8265 (Fig. 2a)²³. Further, we define the minimal convex hull of high traffic locations as the "traffic highland", and through the LISA (Local Indicator of Spatial Association) index (Fig. 2b)²⁴ which gives the "high-high" autocorrelation regions, and spatially clustering using DBscan²⁵, we find in our case that the detected traffic highlands do meet the scale requirements, and they only account for 13.08% of the total study area while capturing 63.68% of the total traffic (Fig. 2c).

The second prerequisite is the temporal stability of the above spatial distribution patterns of traffic. In particular, for operational concerns, we focus on the stability of the traffic highlands during certain practically meaningful time periods (e.g., "working hours"). Note that here temporal stability does not require the absolute stability of traffic in each cell, which is obviously impossible. Instead, what matters is the relative traffic ranking among the cells along time, i.e., whether the traffic highlands at one moment still be highlands at the next. A rank clock analysis²⁶ which yields the ranking of hourly traffic of all cells during a week reveals that among the 168 cells in traffic highlands, more than 150 of them ranked high in all time of the week (occupying the central part of the rank clock) (Fig. 2d). Specifically, although their absolute ranking fluctuated at different times, more than 80% of the traffic highland cells are consistently among the top 168 during more than 80% of the time, with the remaining 20% of the time periods majorly between 3:00 and 6:00 a.m. when traffic usage is low and has no significant energy savings challenges anyway. Similarly, the traffic "lowlands", although also experiencing fluctuations in ranking, remained lowlands at all times. Moreover, we observe in the rank clock that there seems to be an

insurmountable gap between the highland and the non-highland cells, implying that the traffic "highland" is indeed stable over time.

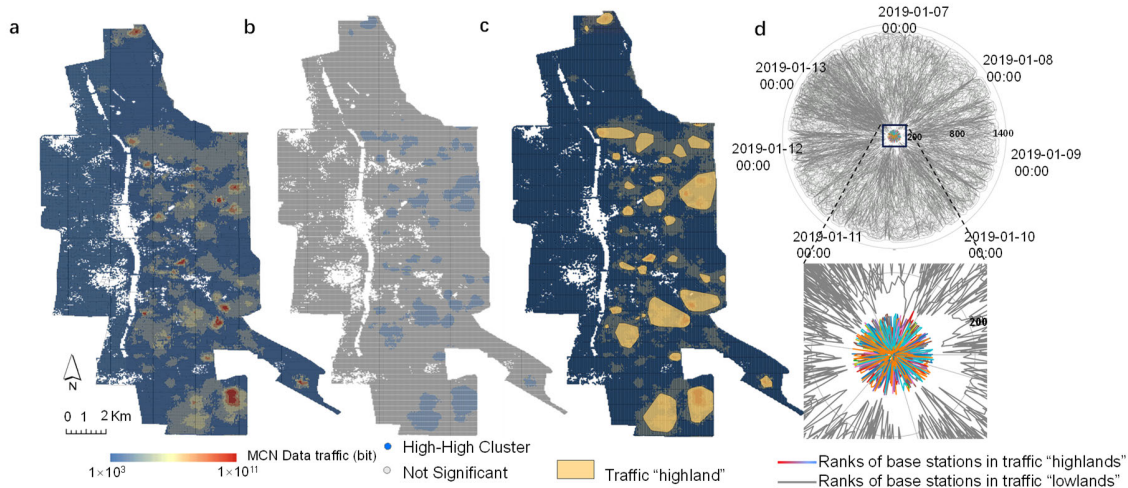


Fig. 2 The spatiotemporal distribution of MCN traffic in Taiyuan

a Spatial distribution of traffic;

b Spatial distribution of high-high local autocorrelation locations of traffic;

c Traffic "highlands" based on spatial cluster of high-high locally autocorrelated locations;

d Rank clock of traffic within a week, where the first-ranked traffic location is in the center of the clock and the lower-ranked locations outwards. The gray lines indicate the traffic "lowland" and the colored lines the traffic "highland" locations.

Spatial optimization through supply-demand coupling of MCN resources for energy-saving

Finally, we estimate the potential effect of an MCN energy saving strategy through spatial optimization. Conceptually, this is achieved by spatially coupling the supply and demand of MCN

resources, such that more base stations are allocated for high traffic areas as the “capacity” layer^{27 28} of the cellular network, and less for the traffic lowland only to ensure basic service coverage. In this picture, ideally the pdf of the traffic distribution should show a single-peak pattern, with fewer base stations covering both very low and very high traffic areas at the head (low-traffic) and the tail (high-traffic) of the distribution, and more in the middle part. This is because, if the probability density of the head was large, one can reduce energy consumption by shutting down the base stations with very low loads and shifting their loads to others nearby; while at the tail of the distribution, we know from previous empirical findings that they only occupy a small portion of the city space, and therefore only a small number of base stations should serve. Fig. 3(c) shows the status quo traffic distribution at the cell level, and one can see that its pdf follows an exponential distribution. In other words, there exists a large number of low-load base stations, and they are undoubtedly the source of low energy efficiency. The supply-demand coupling of MCN resources, i.e., equalizing the spatial distribution of base stations according to the spatial distribution of traffic, should make the two match with each other.

Here, a challenge is that while the citywide spatial distribution of traffic obeys a steep power-law distribution, the pattern cannot be directly extrapolated to smaller scales (Table 1). That is, we cannot follow the pattern of power-law distribution at all spatial scales to simply calculate the proportion of high traffic areas and, consequently, estimate the energy-saving potential. Therefore, we propose a simplified spatial optimization model for energy savings estimation. The model has an objective of minimizing the total energy consumption of all base stations $\sum_i P_i$. With the location of base stations as the decision variable, it optimizes the locations such that the supply of MCN resources matches the geographical pattern of traffic demand. Hence, the model can be technically transformed as a modified maximum set-cover problem²⁹: the traffic coverage $\sum_{i \in I} y_i$ is maximized with a proper set of base station locations, which is subject to a series of constraints regarding the service coverage radius of the base stations, signal strength, along with other technical constraints (See the Methods section for details of the optimization model).

First, for the primary set of experiments, we take the entire study area as the solution space, and solve the problem under two scenarios: 1) holding the number of existing base stations unchanged and only optimizing their locations; and 2) optimizing both the number and location of base stations. The results are shown in Figures 3 and 4, respectively, where for the ease of comparison with the later experimental results, we only show in Fig. 3a and 4a the location of base stations in the traffic highlands as previously identified (see Section B in Supplementary Information for the complete results). A closer look shows that after optimization, the base station locations within traffic highlands are intuitively more consistent with high traffic areas (Fig. 3b, Fig. 4b); the pdf of the base station-level traffic moves right, indicating a reduction in low-load base stations, although the expected one-peak distribution did not emerge because the geographically global optimization would require certain numbers of low-load base stations for necessary service coverage (Fig. 3c, Fig. 4c). In terms of energy-saving effect, calculating using the power parameters of a typical 4G (LTE 2T2R) base station³⁰, the total status quo power of the MCN is 998,600W; while those in the two scenarios are 950,029W (4.86% energy savings) and 751,675W (24.73% energy savings), respectively. The figures, especially the latter, compare favorably with the energy savings obtained by the currently mainstream temporal shutdown operations¹¹⁻¹³. Besides, an examination of the results shows that the load at any base station does not exceed 60%, implying that the increased loads in certain base stations do not affect the user experience due to network congestion, thus supporting the feasibility of the optimization.

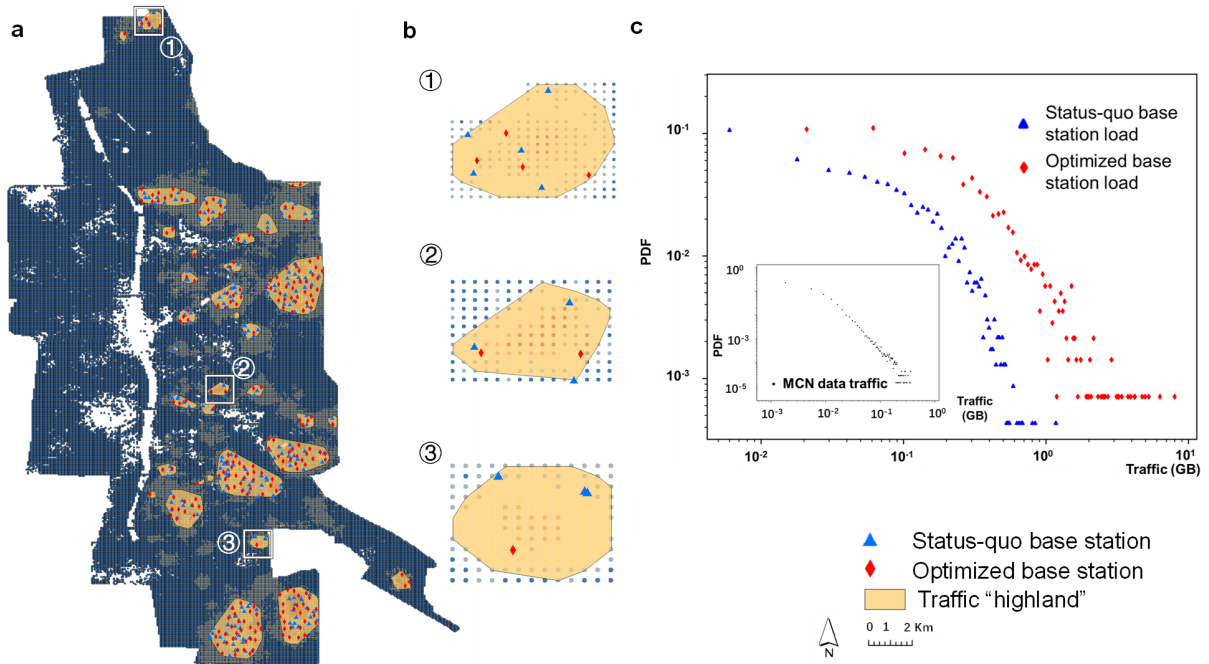


Fig. 3 Energy-saving optimization results with the entire study area as solution space and holding the number of base stations unchanged

a Spatial distribution of original and optimized locations of base stations within the traffic highlands;

b A zoomed-in view of the original and optimized base station locations against traffic distribution in three typical traffic highlands, where it can be found that the optimized base station locations are closer to traffic hotspots;

c Probability density distribution of traffic.

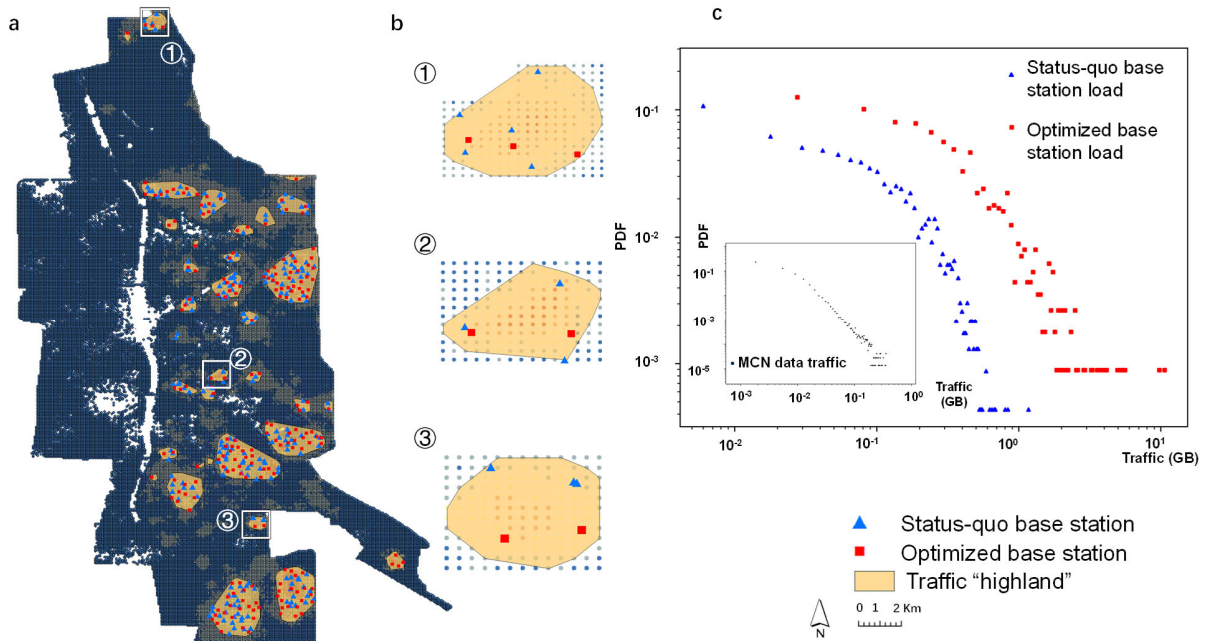


Fig. 4 Energy-saving optimization results with the entire study area as solution space and both the number and location of base stations optimized

a Spatial distribution of original and optimized locations of base stations within the traffic highlands;
b A zoomed-in view of the original and optimized base station locations against traffic distribution in three typical traffic highlands, where it can be found that less base stations are needed and the optimized base station locations are closer to traffic hotspots;
c Probability density distribution of traffic.

Next, considering the existence of the stable traffic highland, we tried to use only the highland as the solution space and conducted the second set of experiments under the same other conditions as the first set of experiments. The results are shown in Figs. 5 and 6, where the total power of the optimized MCN is 973,966W and 802,907W, corresponding to 2.46% and 19.59% energy savings, respectively for the two scenarios. The energy savings do not differ much from those of the first set of experiments. However, the pdf of traffic shows an one-peak pattern in the optimized scenario as expected, i.e., it is no longer

exponential but log-normal due to the drastic reduction of the number of low-load base stations, indicating that the energy efficiency within the traffic highlands is considerably improved. Also, the time costs of solving the problems reduced significantly. The computation time in the first set of experiments for the two scenarios is 176.31s and 32.01s, respectively, in comparison to 12.63s and 3.31s in the second set of experiments. It can be seen that the second set of experiments, which solves only for the traffic highlands, achieves more than an order of magnitude improvement in computational efficiency, while the corresponding loss in energy efficiency is only 20% (for the second scenario).

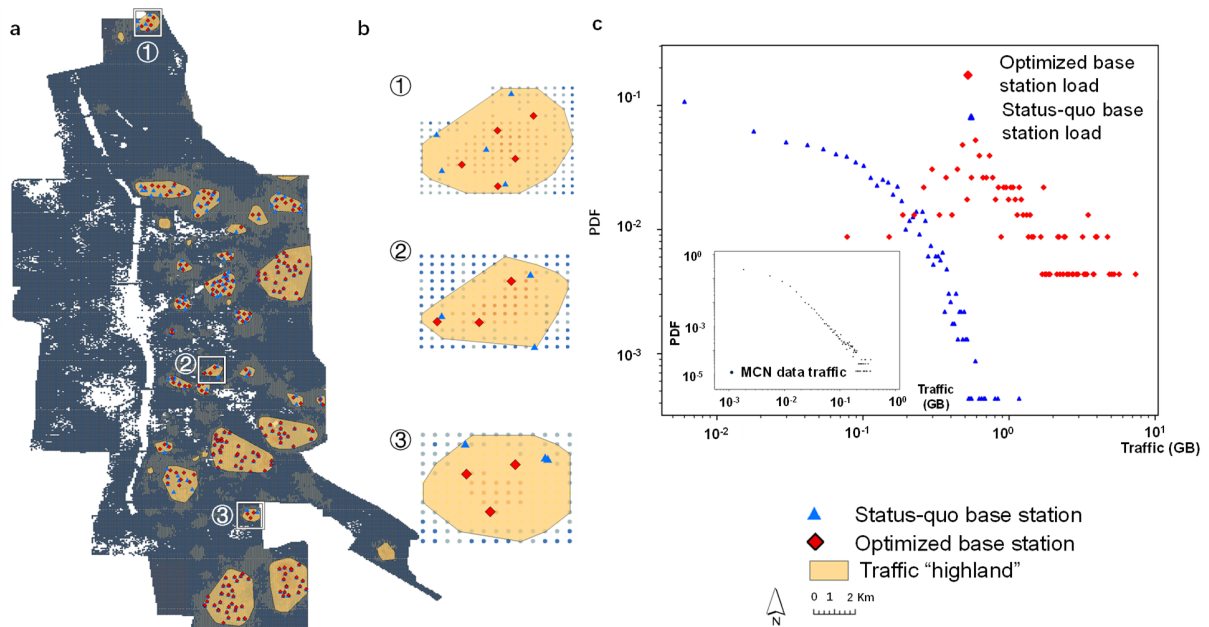


Fig. 5 Energy-saving optimization results with the *traffic highlands* as solution space and holding the number of base stations unchanged

a Spatial distribution of original and optimized locations of base stations within the traffic highlands;

b A zoomed-in view of the original and optimized base station locations against traffic distribution in three typical traffic highlands, where it can be found that the optimized base station locations are closer to traffic hotspots;

c Probability density distribution of traffic.

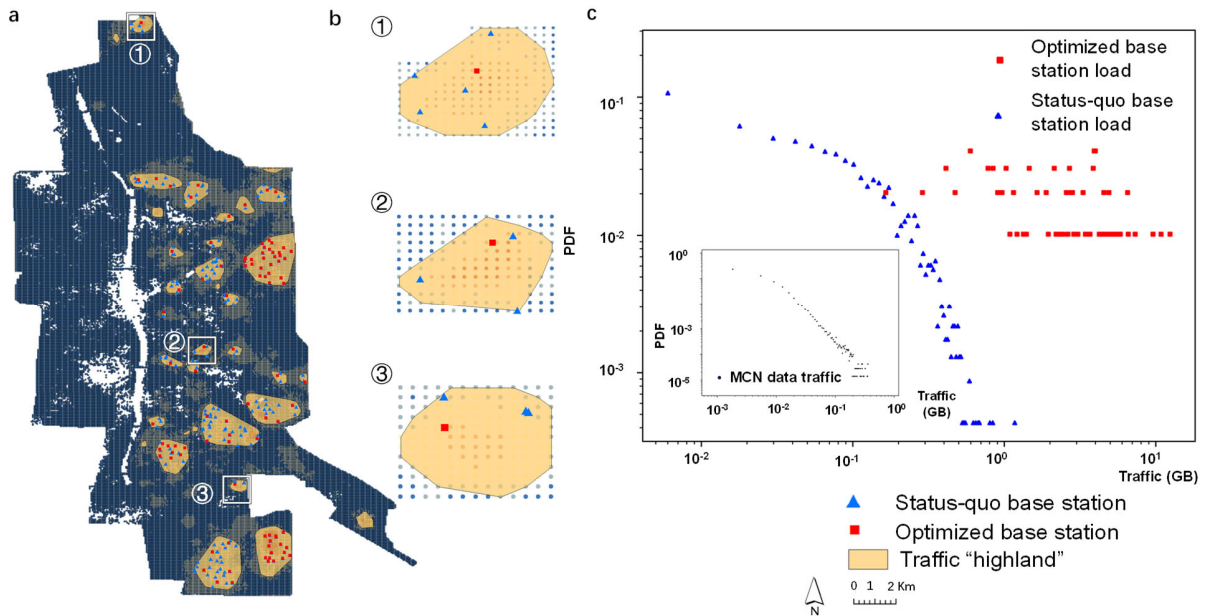


Fig. 6 Energy-saving optimization results with the *traffic highlands* as solution space and both the number and location of base stations optimized

- a* Spatial distribution of original and optimized locations of base stations within the traffic highlands;
- b* A zoomed-in view of the original and optimized base station locations against traffic distribution in three typical traffic highlands, where it can be found that less base stations are needed and the optimized base station locations are closer to traffic hotspots;
- c* Probability density distribution of traffic.

Moreover, besides the above experiments which use the technical parameters of the 4G network, we perform the third set of experiments using 5G parameters, of which major changes involve the service coverage radius and power of individual base stations, and we set the former to 150 m and the latter according to literature ¹². Also, since the 5G scenario is a counterfact and there is no real-world baseline, we refer to the popular rough estimation of the energy consumption of 5G networks as cited earlier as the

baseline for comparison, which assumes that each 4G base station cell requires three 5G base station cells to achieve the same coverage. The total power of the 5G base stations hence estimated at the baseline is 2356.875 KW; as a comparison, the total power, after optimizing both the number and location of base stations, is 1657.353 KW, i.e., an energy saving of 29.68% is obtained (Fig. 7).

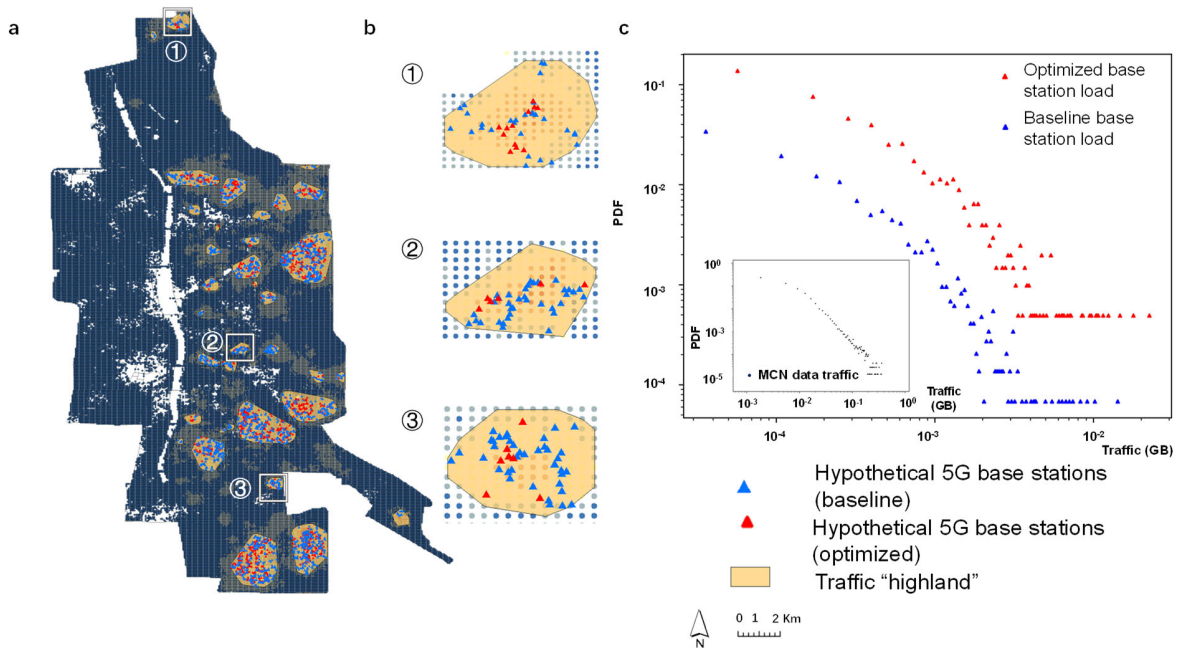


Fig. 7 Energy-saving optimization results for a hypothetical 5G MCN

a Spatial distribution of original and optimized locations of base stations within the traffic highlands;

b A zoomed-in view of the original and optimized base station locations against traffic distribution in three typical traffic highlands, where it can be found that the optimized base station locations are closer to traffic hotspots;

c Probability density distribution of traffic.

Discussion

It should be noted that the estimated energy saving potentials in this paper are subject to both over and under estimations. On the one hand, in the real world, especially in urban environments, the real service coverage radius of base stations does not always reach the theoretical maximum due to building shading and other reasons, and the resulting need for additional base stations would make the actual energy saving benefit lower compared to our simplified calculations. On the other hand, limited by the spatial resolution of the raw data, we actually do not know the ground truth of spatial distribution of traffic at a smaller spatial resolution than the cell level. The data used in this paper, as the telecom operator preprocessed it, distributed the cell-level traffic equally among all analysis units (the 50 * 50m grids) within its coverage. However, both the maximum entropy derivation and the empirical calculations in Table 1 would imply that the actual traffic distribution is still likely to be highly skewed at a very small scale. Therefore, it is likely that the traffic data used in this paper actually underestimated the skewness of the traffic distribution for its relatively grain-corased granularity, leading to an underestimation of the energy saving potential. On balance, although we do not know whether the two errors can cancel each other out, we can at least be assured that the results are not one-way biased.

The potential energy savings from the strategy proposed in this paper, which follows a spatial optimization approach, are several times better than the currently widely used temporal shutdown-based measures³¹. Moreover, the spatial optimization approach has significant advantages from the operational point of view. This is because, unlike the temporal shutdown measures, which relies on the prediction of real-time, wide-area traffic, the spatial optimization approach is based on the stable pattern of traffic distribution. Therefore, it is a once-and-for-all task over a reasonable time span. Besides, technically, changes in the spatial coverage of MCN resources in 5G networks can be realized using the beam-forming technology⁴ without the need for large-scale physical rearrangement of existing base stations, which enhances the strategy's feasibility.

The empirical results in this paper show a power-law spatial distribution of traffic at the citywide scale, along with power-law or exponential distributions at smaller scales (Fig. 8a). Interestingly, the spatial distribution of the population itself, as the user of the telecom service, is also found to have a similar scaling pattern^{18,19}; and at large scales, the power parameters of both population and traffic distributions appear to be close to 2³². As the spatial distribution of traffic can be viewed as that of the population after certain behavior mapping, the coincidence seems to imply that the mapping may have a simple form, which is an interesting direction of future investigation.

Another interesting finding is the heterogeneity of the spatial distribution forms of traffic. Our findings show that at the same spatial scale, the spatial distribution of traffic in different areas of the city exhibit different forms (Fig. 8b, c). We speculate that the heterogeneity essentially derives from the same characteristics of the spatial distribution of mobile users, which in turn are related to the spatial heterogeneity of the city's functions and structures. Specifically, various parts of urban areas, or urban places at different scales, have different functional combinations and spatial forms. As different urban places may have different activating or inhibiting effects on people's traffic usage, the spatial distribution of traffic should reasonably have diversified forms. Nevertheless, if some small-scale urban places happen to have an mixture of urban functions and forms that are similar to those of the entire city, their traffic distribution may also exhibit similar characteristics to those of the city as a whole. This conjecture seems to explain the empirical findings in Table 1. While the revelation of the skewed spatial distribution pattern of traffic in this paper is sufficient to establish the basis for the strategy of achieving MCN energy savings through spatial optimization, it is still of great interest to reveal the root of this form of distribution. From the above discussion, it appears that the phenomenon is essentially a manifestation of the classical Modifiable Areal Unit Problem (MAUP)²¹ in geography. Therefore, a deeper investigation of this problem may need to be supported by additional findings from urban science, as well as studies on the behavioral patterns of human mobility and traffic usage.

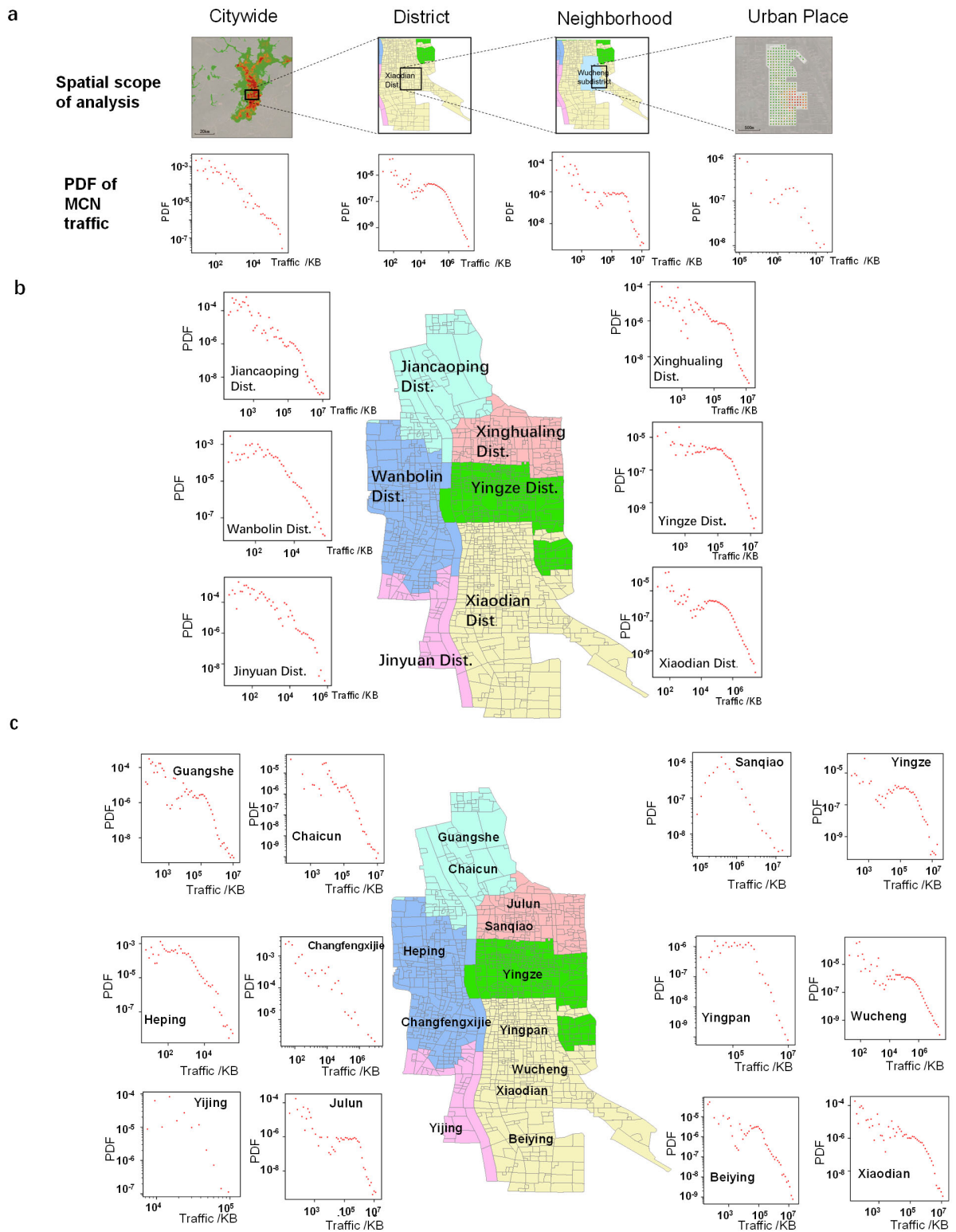


Fig. 8 The scaling and spatial heterogeneous characteristics in the spatial distribution of traffic

a The spatial scaling patterns of the probability density distribution of traffic;

b The spatial heterogeneity patterns of the probability density distribution of traffic at the jurisdictional district level;

c The spatial heterogeneity patterns of the probability density distribution of traffic at the jurisdictional subdivision level.

Finally, in an operational sense, the findings of this paper on the persistence of stable traffic highlands hint at the potential advantages of using local rather than global solution in energy-efficient optimization of the MCN. Experiments show that the local approach with only the traffic highlands as the solution space obtains a computational efficiency improvement higher than one order of magnitude with less than 20% loss of optimization benefit compared to the global solution approach, and thus has a significant advantage in terms of cost-efficiency. Considering the high requirement for agility in real-world energy-efficient optimization of the MCN ³³, the result highlights the important operational significance of traffic highland identification in practice.

Methods

Maximum entropy-based derivation of the spatial distribution form of traffic

By the maximum entropy assumption, the spatial distribution function $P(X)$ of the traffic should satisfy the following conditions:

$$\begin{aligned} \min \quad & \sum_k P(X = k) \cdot \ln P(X = k) \\ \text{s. t.} \quad & \sum_k P(X = k) = 1 \\ & \sum_k P(X = k) \cdot c(k) = a \end{aligned} \quad (2)$$

Where $P(X = k)$ is the probability when the random variable X for the value of the traffic (in bits) takes the value k . The first of the two constraints is a straightforward aggregate constraint. The second constraint introduces the traffic affine function $c(k)$, which gives the number of people (users) in the spatial location where $X = k$. Referring to previous studies on the relationship between traffic and population¹⁷, we can reasonably assume that such mapping relationship exists. Therefore, the second constraint implies that the expectation of the population distribution in the city is convergent, which has been tested by previous studies³⁴.

Constructing the Lagrangian function for the solution, we obtain:

$$P(X = k) = e^{\lambda_0 - 1 + \lambda_1 \cdot c(k)} \quad (3)$$

Where the specific form of $c(k)$ is unknown. Nevertheless, based on findings in the urban science on the spatial distribution pattern of the urban population^{34,35}, and considering the heterogeneity of the urban space³⁶⁻³⁸, we can conjecture several possible forms of $c(k)$. Depending on its skewness, we assume that $c(k)$ is logarithmically, linearly, power-law, Poisson, exponentially, and Gaussian distributed (see Section A in Supplementary Information for proof of convergence), and the respective solutions are:

$$P(X = k) = \begin{cases} e^{\lambda_0-1} k^{\lambda_1}; c(k) = \ln k \\ e^{\lambda_0-1} e^{\lambda_1 \cdot k}; c(k) = ak + b \\ e^{\lambda_0-1+\lambda_1 k^{-w}}; c(k) = k^{-w} \\ e^{\lambda_0-1+\lambda_1 e^{-t} \frac{t^k}{k!}}; c(k) = e^{-t} \frac{t^k}{k!} \\ e^{\lambda_0-1+\lambda_1 \cdot e^{-k}}; c(k) = e^{-k} \\ e^{\lambda_0-1+\lambda_1 \frac{1}{\sqrt{2\pi\sigma}} e^{-\frac{k^2}{2\sigma^2}}}; c(k) = \frac{1}{\sqrt{2\pi\sigma}} e^{-\frac{(k-\mu)^2}{2\sigma^2}} \end{cases} \quad (4)$$

It can be seen that the form of $P(X = k)$ in the first case is a power-law distribution, and is exponential in the second; those in other cases are complex in form, but they can all be considered certain variations of generalized exponential distributions. Clearly, as the skewness of $c(k)$ increases, $P(X = k)$ changes from a power-law distribution to other forms of probability density distribution, and the skewness of all these forms are much higher than that of the power-law distribution. This means that among the possible forms of $c(k)$, the corresponding $P(X = k)$ distribution is at least power-law and may take on a more long-tailed distribution form. In terms of the energy saving potential incubated in such form of traffic distribution, a power-law form is “good” enough, while the others breeds much larger energy saving potential.

MCN base station energy saving optimization problem statement

The base station in a 4G cellular network is an access link between the core network and the mobile devices (users). A base station consists of a set of equipments including power amplifiers, baseband units, RF units, power supplies, and air conditioning. The power of a base station in operation in a 4G cellular network P_{Op} is ³⁰.

$$P_{Op} = N_{TRX} \times [P_{PA}^{DC} + P_{RF}^{DC} + P_{BB}^{DC}] / (1 - \sigma_{DC})(1 - \sigma_{cool}) \quad (5)$$

Where N_{TRX} denotes the number of transceivers in the base station; P_{PA}^{DC} denotes the power of the power amplifier module; P_{RF}^{DC} denotes the power of the RF unit; P_{BB}^{DC} denotes the power of the baseband unit; and σ_{DC} and σ_{cool} denote the power loss of DC boost and air conditioning cooling, respectively, which take the values of 6% and 10%, respectively by general industry standards.

P_{PA}^{DC} is a linear function of the base station transmit power P_{tx}^{max} . Denoting the amplifier efficiency with η_{PA} , we have:

$$P_{PA}^{DC} = P_{tx}^{max} / \eta_{PA} \quad (6)$$

In general, both coverage and signal propagation attenuation are considered to be the main factors in determining the transmitting power of a base station. A simplified formula is expressed as follows:

$$P_{tx}^{max} = P_0 (R/R_0)^a \quad (7)$$

Where a denotes the signal propagation path attenuation coefficient; R_0 denotes the standardized coverage radius of the base station with the standardized radius of 1 km; P_0 denotes the standardized power of the base station with the standardized power of 40 W.

Lastly, in addition to the operational power P_{op} , the base station includes a microwave antenna connecting the base station to the core network which has the power of P_{mc} , and a lighting module with the power of P_{lm} ³⁰. Thus, the total power of an LTE-macro base station is:

$$P_{BS} = \frac{N_{TRX} \times \left(\frac{P_0 \left(\frac{R}{R_0}\right)^a}{\eta_{PA}} + P_{RF}^{DC} + P_{BB}^{DC} \right)}{(1 - \sigma_{DC})(1 - \sigma_{cool})} + P_{mc} + P_{lm} \quad (8)$$

Hence, holding operational time and the number of base stations constant, the optimization problem of base station distribution for minimizing energy consumption can be stated as follows:

$$\min: \sum_i P_i \quad (9)$$

$$s. t. SINR_k \geq SINR_{th}, \forall k = 1, 2, \dots, N_u; \quad (10)$$

$$P_i \leq P_{max} \quad (11)$$

Where:

$$\begin{aligned} SINR_k &= \frac{P_{re,k}}{I_{out,k} + \delta^2} \\ P_{re,k} &= \sum_{m=1}^S P_{b_{m,k}} g_{b_{m,k},k} \\ I_{out,k} &= \sum_{i=1, i \neq b_{m,k}}^{N_b} P_i g_{i,k} \\ g_{i,k} &= (D_{i,k})^{-\alpha} L_0 \\ P_i &= \sum_k P_{i,k} \\ P_{i,k} &= P_{BBU} + P_{RRU_0} + \beta T_{i,k} \\ b_{m,k} &= \{i | D_{b_{m,k}} = \min\{D_{1,k}, D_{2,k}, \dots, D_{N_b,k}\}\} \end{aligned} \quad (12)$$

Where P_i denotes the power of base station i . The two constraint terms include the signal strength constraint and the power rating constraint. Specifically, for the first constraint, $SINR$ denotes the signal-to-noise ratio at user k , which is equal to the ratio of the received base station transmit power at user k ($P_{re,k}$) to the sum of the received interference power at user k ($I_{out,k}$) and the ambient noise δ^2 , where $P_{re,k}$ is equal to the product of the transmit power of the closest base station at user k ($P_{b_{m,k}}$) and the transmit loss ($g_{b_{m,k},k}$), the latter of which is related to the transmit distance $D_{i,k}$ and the path loss factor L_0 ; and $I_{out,k}$ denotes weak signal interference base station power received at user k . For the second constraint, P_i is the sum of $P_{i,k}$ at all locations k , which is the power consumed by base station i for the traffic provided to location k , and can be computed as the sum of the baseband unit power (P_{BBU}), the RF

unit base power (P_{RRU_0}), and the power for transmitting data packets $\beta T_{i,k}$. The coefficient β describes the relationship between traffic volume and the respective power^{39,40}. And P_{max} is the power rating of the base station. Note that we did not explicitly include the load of base stations in the optimization problem, as in real-world MCN operations the factor rarely exceeds 30%, and thus does not affect the user experience of MCN services. However, we do validate that the factor does not exceeds a reasonable level in our results.

When discretizing the solution space with a 50 * 50m grid, and holding the number of base stations as is in the status quo, the above optimization problem can be transformed into an integer programming problem:

$$\max \sum_{i \in I} y_i \quad (13)$$

$$s. t. y_i \in \{0, 1\}, i \in I \quad (14)$$

$$x_j \in \{0, 1\}, j \in J \quad (15)$$

$$\sum_{j \in J} x_j = N_b \quad (16)$$

$$\sum_{j \in N_i} x_j \geq y_i, N_i = j \in J: d_{i,j} \leq R \quad (17)$$

Where y_i denotes the required coverage locations in the location space I , and $\{0, 1\}$ represents whether a location is covered; x_j denotes possible base station locations in the location space J , and $\{0, 1\}$ represents whether a location is chosen. N_b denotes the number of base stations in the result. $d_{i,j}$ denotes the distance between i and j . And R represents the base station coverage area.

Further, when the number of base stations (N_b) is also optimized, the original optimization objective is stated as (with the constraints unchanged):

$$\min: \begin{cases} \sum_i P_i \\ N_b \end{cases} \quad (18)$$

We now have to filter out the unnecessary base stations. And the integer programming problem now can be stated as:

$$\min \sum_{i \in I} x_i \quad (19)$$

$$s. t. x_i \in \{0, 1\}, i \in I \quad (20)$$

$$\sum_{j \in N_{i,j}} x_i \cdot y_j \leq C, N_{i,j} = \{j | d_{i,j} \leq d_{p,j}, \text{ for } p \text{ in } I\} \quad (21)$$

$$\sum_{i \in I} x_i \cdot D_{i,j} \geq 1, \text{ for } j \in J \quad (22)$$

$$D_{i,j} \begin{cases} 0, d_{i,j} > R \\ 1, d_{i,j} \leq R \end{cases} \quad (23)$$

The additional constraints are necessary because we have to keep the traffic load of a base station under its capacity, which is directly related to the service coverage radius R of the base station. The specific value of R is related to the terrain status of the service area, and in this paper we take a 300m value for the 4G network and 150m for the 5G network, which are drawn from experience ⁴¹.

Data

The MCN traffic data used in this paper are for the urban area of Taiyuan, the capital of Shanxi Province, China (a map of the study area is available in Section C in Supplementary Information), from

January 7, 2020 to January 17, 2020, with an hourly temporal resolution and cell-level spatial resolution. The original data includes information on upstream and downstream traffic values, number of users, and MCN signal strength in each cell. The data has been resampled to have a 50 * 50m spatial resolution by the data provider (the telecom operator) through evenly distributing the traffic of a cell among its coverage area.

Data Availability

The original data of MCN traffic used in this paper is temporarily not publicly available by data provision terms from the data provider.

Code Availability

The model and code used in this study are available upon request.

References

1. Raymond, P. A. *et al.* Global carbon dioxide emissions from inland waters. *Nat.* 2013 5037476 **503**, 355–359 (2013).
2. van Eyden, R., Difeto, M., Gupta, R. & Wohar, M. E. Oil price volatility and economic growth: Evidence from advanced economies using more than a century's data. *Appl. Energy* **233–234**, 612–621 (2019).
3. Sturm, C. Between a rock and a hard place: European energy policy and complexity in the wake of the Ukraine war. *J. Ind. Bus. Econ.* 1–44 (2022) doi:10.1007/s40812-022-00233-1.
4. Han, S. & Bian, S. Energy-efficient 5G for a greener future. *Nat. Electron.* **3**, 182–184 (2020).
5. Dabaghi, F., Movahedi, Z. & Langar, R. A survey on green routing protocols using sleep-scheduling in wired networks. *J. Netw. Comput. Appl.* **77**, 106–122 (2017).

6. Chen, J., Ge, X. & Ni, Q. Coverage and handoff analysis of 5g fractal small cell networks. *IEEE Trans. Wirel. Commun.* **18**, 1263–1276 (2019).
7. Soh, Y. S., Member, S., Quek, T. Q. S. & Member, S. Energy Efficient Heterogeneous Cellular Networks. **31**, 840–850 (2013).
8. White, M. J. Segregation and diversity measures in population distribution. *Popul. Index* (1986) doi:10.2307/3644339.
9. Yu, F. *et al.* Cutting without pain: Mitigating 3G radio tail effect on smartphones. in *2013 Proceedings IEEE INFOCOM* 440–444 (IEEE, 2013). doi:10.1109/INFOCOM.2013.6566811.
10. Holtkamp, H., Auer, G., Bazzi, S. & Haas, H. Minimizing Base Station Power Consumption. *IEEE J. Sel. Areas Commun.* **32**, 297–306 (2014).
11. Debaille, B., Desset, C. & Louagie, F. A Flexible and Future-Proof Power Model for Cellular Base Stations. in *2015 IEEE 81st Vehicular Technology Conference (VTC Spring)* vol. 2015 1–7 (IEEE, 2015).
12. Lahdekorpi, P., Hronec, M., Jolma, P. & Moilanen, J. Energy efficiency of 5G mobile networks with base station sleep modes. *2017 IEEE Conf. Stand. Commun. Networking, CSCN 2017* 163–168 (2017) doi:10.1109/CSCN.2017.8088616.
13. Salahdine, F. *et al.* A survey on sleep mode techniques for ultra-dense networks in 5G and beyond. *Comput. Networks* **201**, 108567 (2021).
14. Miller, H. J. A Measurement Theory for Time Geography. *Geogr. Anal.* **37**, 17–45 (2005).
15. Hägerstrand, T. WHAT ABOUT PEOPLE IN REGIONAL SCIENCE? *Pap. Reg. Sci.* **24**, 7–24 (1970).
16. Oh, E., Son, K. & Krishnamachari, B. Dynamic base station switching-on/off strategies for green cellular networks. *IEEE Trans. Wirel. Commun.* **12**, 2126–2136 (2013).
17. Douglass, R. W., Meyer, D. A., Ram, M., Rideout, D. & Song, D. High resolution population estimates from telecommunications data. *EPJ Data Sci.* **4**, 1–13 (2014).
18. Zipf, G. K. The P1P2 / D Hypothesis : On the Intercity Movement of Persons Author (s): George Kingsley Zipf Source : American Sociological Review , Vol . 11 , No . 6 (Dec . , 1946), pp . 677-686 Published by : American Sociological Association Stable URL : http://. *Am. Sociol. Rev.* **11**, 677–686 (1946).
19. Xi, L. The Empirical Research on China’s City Size Distribution: An Exploration Based on the Micro Spatial Data and City Clustering Algorithm. *J. Zhejiang Univ. Soc. Sci.* **45**, 120–132 (2015).
20. Wilson, A. G. Inter-regional Commodity Flows: Entropy Maximizing Approaches. *Geogr. Anal.* **2**, 255–282 (1970).
21. Openshaw, S. *The modifiable areal unit problem. Quantitative geography: A British view* (Routledge and Kegan Paul, Andover, 1981).

22. Goodchild, M. F. The validity and usefulness of laws in geographic information science and geography. *Ann. Assoc. Am. Geogr.* **94**, 300–303 (2004).
23. MORAN, P. A. Notes on continuous stochastic phenomena. *Biometrika* **37**, 17–23 (1950).
24. Anselin, L. Local Indicators of Spatial Association—LISA. *Geogr. Anal.* **27**, 93–115 (1995).
25. Atluri, G., Karpatne, A. & Kumar, V. Spatio-Temporal Data Mining: A Survey of Problems and Methods. *ACM Comput. Surv.* **51**, (2017).
26. Batty, M. Rank clocks. *Nature* **444**, 592–596 (2006).
27. Aliu, O. G., Imran, A., Imran, M. A. & Evans, B. A survey of self organisation in future cellular networks. *IEEE Commun. Surv. Tutorials* **15**, 336–361 (2013).
28. Buenestado, V., Toril, M., Luna-Ramírez, S., Ruiz-Avilés, J. M. & Mendo, A. Self-tuning of remote electrical tilts based on call traces for coverage and capacity optimization in LTE. *IEEE Trans. Veh. Technol.* **66**, 4315–4326 (2017).
29. Clarkson, K. L. & Varadarajan, K. Improved Approximation Algorithms for Geometric Set Cover. *Discrete Comput. Geom.* **37**, 43–58 (2007).
30. Alsharif, M. H. & Kim, J. Optimal solar power system for remote telecommunication base stations: A case study based on the characteristics of south Korea’s solar radiation exposure. *Sustain.* **8**, (2016).
31. Marsan, M. A., Chiaraviglio, L., Ciullo, D. & Meo, M. Optimal energy savings in cellular access networks. *Proc. - 2009 IEEE Int. Conf. Commun. Work. ICC 2009* 1–5 (2009)
doi:10.1109/ICCW.2009.5208045.
32. Schläpfer, M. *et al.* The universal visitation law of human mobility. *Nature* **593**, 522–527 (2021).
33. Xu, Y., Yin, F., Xu, W., Lin, J. & Cui, S. Wireless Traffic Prediction with Scalable Gaussian Process: Framework, Algorithms, and Verification. *IEEE J. Sel. Areas Commun.* **37**, 1291–1306 (2019).
34. Batty, M. Space, Scale, and Scaling in Entropy Maximizing. *Geogr. Anal.* **42**, 395–421 (2010).
35. Jiang, B. & Jia, T. Zipf’s law for all the natural cities in the United States: A geospatial perspective. *Int. J. Geogr. Inf. Sci.* **25**, 1269–1281 (2011).
36. Tobler, W. R. A Computer Movie Simulating Urban Growth in the Detroit Region. *Econ. Geogr.* **46**, (1970).
37. Lee, J. G., Han, J. & Li, X. Trajectory outlier detection: A partition-and-detect framework. *Proc. - Int. Conf. Data Eng.* **00**, 140–149 (2008).
38. Clark, C. Urban Population Densities. *J. R. Stat. Soc. Ser. A* **114**, 490–496 (1951).
39. Gadze, J. D., Aboagye, S. B. & Agyekum, K. A. P. Real Time Traffic Base Station Power Consumption Model for Telcos in Ghana. *Int. J. Comput. Sci. Telecommun.* **7**, (2016).

40. Lorincz, J., Garma, T. & Petrovic, G. Measurements and modelling of base station power consumption under real traffic loads. *Sensors* **12**, 4281–4310 (2012).
41. Paul, U., Subramanian, A. P., Buddhikot, M. M. & Das, S. R. Understanding traffic dynamics in cellular data networks. *Proc. - IEEE INFOCOM* 882–890 (2011)
doi:10.1109/INFOCOM.2011.5935313.

Ethics declarations

Competing interests

The authors declare no competing interest.
